# Supporting Information

# Interactions of Thermochromic Liquid Crystal with Surface-Modified PET Substrates for Thermal Sensing Applications

Sreenivasan Sreenivasan Narayanan[a], Lineth Perez Monsalve[a], Christina Tang[b*], Hong Zhao[a*]

a. Department of Mechanical and Nuclear Engineering, Virginia Commonwealth University, 70S Madison street, Richmond, VA 23220, USA
b. Department of Chemical and Life Science Engineering, Virginia Commonwealth University, Richmond, VA 23284, USA

*To whom correspondences should be addressed:

Tel: 804-827-7025

Email: hzhao2@vcu.edu

Tel: 804-827-1917

Email: ctang2@vcu.edu

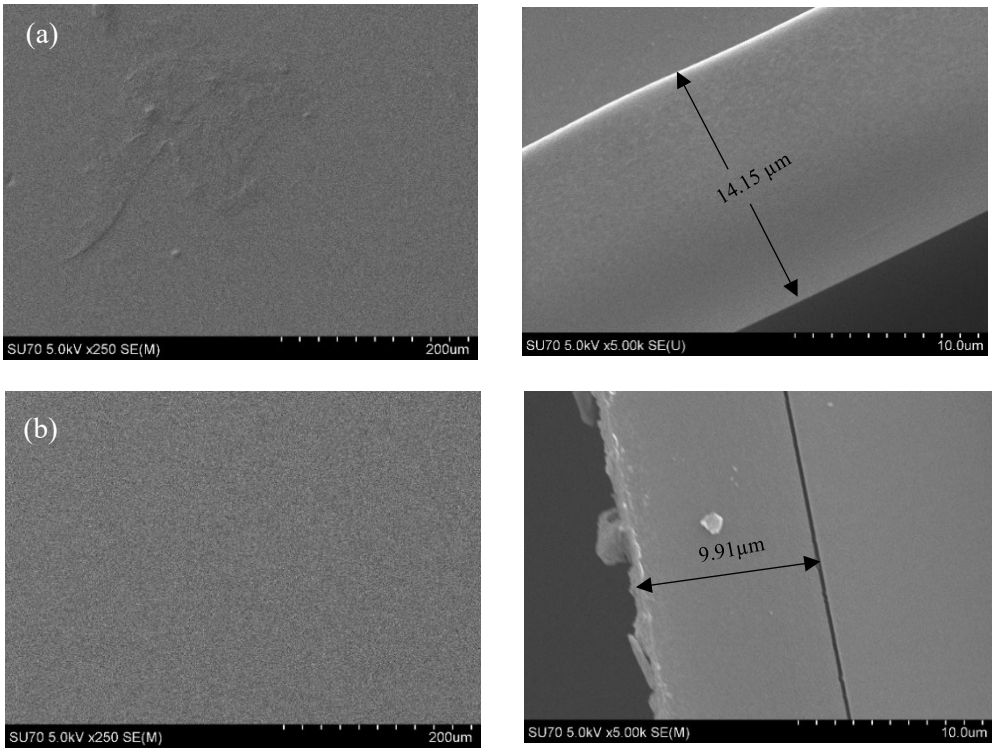


**Figure S1.** SEM images of (a) NeverWet coating on the PET substrate and its thickness on a silicon wafer and (b) PVA coating on the PET substrate and its thickness on a silicon wafer.

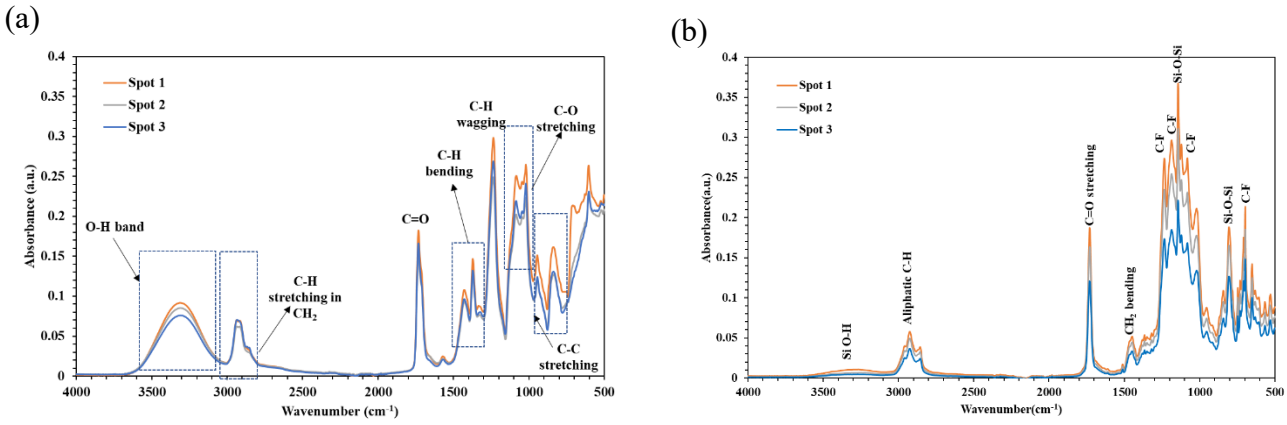


**Figure S2.** FTIR spectra of (a) PVA-coated layer and (b) NeverWet-coated layer.

Attenuated Total Reflectance Fourier Transform Infrared (ATR–FTIR) spectra were collected at three different locations (Spot 1–Spot 3) on each coated surface, to evaluate the spatial uniformity of the coating. The spectra obtained from different spots exhibit highly similar absorption features,

indicating that the coating composition is consistent across the examined region. Minor variations in peak intensity among the spots are attributed to local differences in coating thickness, surface roughness, or ATR contact, rather than changes in chemical composition. **Figure S2** shows the FTIR spectrum of (a) PVA coated layer and (b) NeverWet coated layer. The PVA-coated layer shows the typical PVA fingerprint,[S1,S2] with a broad O–H stretching band around 3200–3600 $cm^{-1}$, along with C–H stretching peaks near 2850–3000 $cm^{-1}$ and a strong C–O stretching region around 1000–1150 $cm^{-1}$, reflecting its hydroxyl-rich polymer structure. In comparison, the NeverWet-coated layer displays clear signatures of a hydrophobic coating,[S3,S4] most notably strong Si–O–Si stretching peaks around 1000–1100 $cm^{-1}$ and distinct C–F stretching bands in the ~1100–1300 $cm^{-1}$ range, consistent with siloxane/fluorinated components.

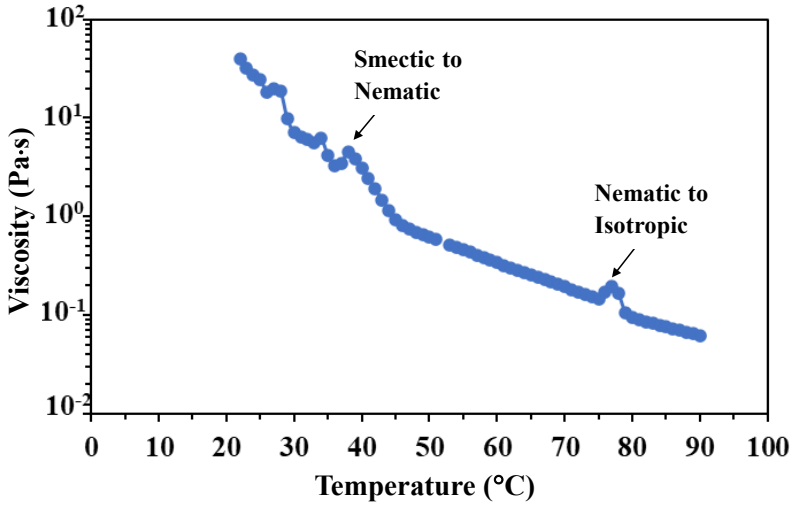


**Figure S3.** Viscosity of CLC ink as a function of temperature.

**Differential Scanning Calorimetry (DSC) characterization of the CLC ink**

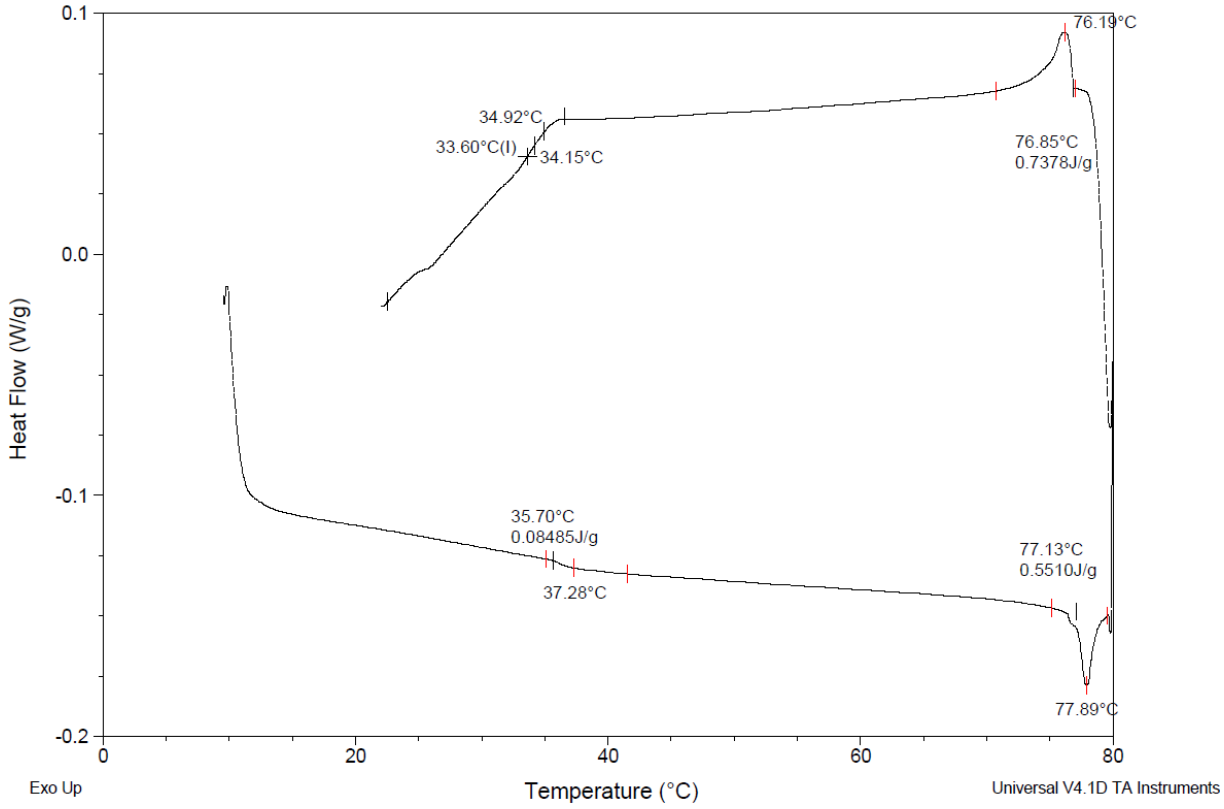


**Figure S4.** Determination of transition temperatures by DSC, 36.1 ± 0.2 ℃ from smectic to nematic phase and 75.2 ± 2.3 ℃ from nematic to isotropic phase.

**Calculation of surface roughness of the CLC coating films**

The surface roughness of the coated CLC films was measured using a Nikon Eclipse LV100D optical microscope equipped with the imaging software. Samples were mounted flat on glass slides and imaged in reflection mode at 20× magnification. A Z-stack (extended depth of focus) was acquired over representative regions of interest using a suitable step size (0.5–1.0 µm for 20×), followed by 3D surface reconstruction.

Using the following equation, RMS roughness was calculated from the reconstructed height map along the specified line shown in Figure 3. It is worth noting that prior to roughness calculation, first-order leveling was applied to eliminate systematic error due to sample tilt.

$$RMS = \sqrt{\frac{1}{K}\sum_{k=1}^{K}(z_k - \overline{z})^2} \quad (1)$$

Where: $z_k$ is the height at each measured point; $\overline{z}$ is the mean height of the surface; $K$ is the total number of height points.

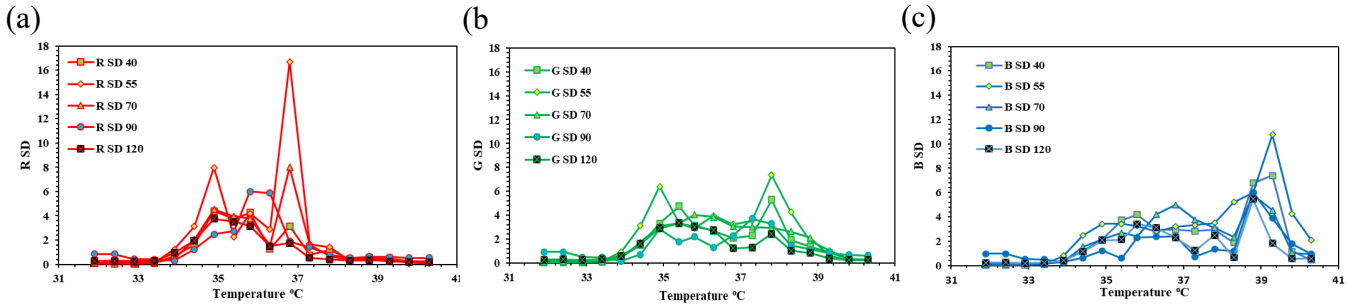


**Figure S5.** Standard deviations (SD) of (a) Red (b) Green and (c) Blue of the CLC films fabricated at different temperatures.

It is not clear why the film coated at 55 °C has much larger variations in the RGB intensities. We do notice that at 40 °C the CLC ink exhibits more liquid-like behavior (G″ > G′) as shown in Figure 2b, while the difference between G″ and G′ diminishes as temperature increases till the transition temperature of ~75 °C. (We have repeated this experiment multiple times; the same trend has been obtained.) At 55 °C, the CLC has G″/G′≈1, which may destabilize flow and shear-induced alignment during the coating process, leading to larger variations. Nevertheless, fundamental studies and characterizations of the CLC ink at the molecular level is needed to fully understand the structure changes as temperature increases.

**Calculation of the surface free energy of a solid surface using OWRK model**

Wetting of a solid surface is an important consideration in the printing industry and is typically assessed using the contact angle (θ), which indicates the angle between the liquid–vapor interface and the solid substrate. Within a material, molecules in the bulk are subject to balanced forces, whereas surface molecules experience an inward force. For solids, this force is termed surface free energy (SFE)—the amount of energy needed to increase the surface area of a material by one square meter. By knowing a material's SFE, one can determine its ability to be wetted by a specific liquid. A solid is considered wettable by a liquid if its SFE is equal to or greater than the surface tension of the liquid.

The surface free energy (SFE) of a solid cannot be measured directly; instead, it is generally estimated using theoretical models. One widely used approach is the Owens-Wendt-Rabel-Kaelble (OWRK) model, a two-component system based on Fowkes' assumption that two different types of interactions take place at the solid–liquid interface.[S5] According to this model, the SFE of solids and the surface tension of liquids are

separated into dispersive and polar components, which are calculated using geometric mean relationships. The interfacial tension between solid and liquid phases, $Y_{SL}$ is:

$$\mathrm{Y}_{SL} = \mathrm{Y}_L + \mathrm{Y}_S - 2\left(\sqrt{\mathrm{Y}_L^D \mathrm{Y}_S^D} + \sqrt{\mathrm{Y}_L^P \mathrm{Y}_S^P}\right) \quad (2)$$

Where $\mathrm{Y_L}$ represents the total surface tension of the liquid, $\mathrm{Y_S}$ denotes the total SFE of the solid, and the superscripts D and P indicate the dispersive and polar components, respectively. Substituting the equation (2) to the Young's equation, $Y_S = Y_{SL} + Y_L cos\theta$, yields:

$$\frac{\mathrm{Y}_L(cos\theta+1)}{2\sqrt{\mathrm{Y}_L^D}} = \sqrt{\mathrm{Y}_S^P}\frac{\sqrt{\mathrm{Y}_L^P}}{\sqrt{\mathrm{Y}_L^D}} + \sqrt{\mathrm{Y}_S^D} \quad (3)$$

Surface free energy (SFE) parameters of a solid surface are determined by measuring the contact angles of at least two reference liquids with known dispersive ($\mathrm{Y}_L^D$) and polar ($\mathrm{Y}_L^P$) components of surface free energy ($Y_L$). A linear regression analysis is then conducted on the plot of ($\mathrm{Y}_L(cos\theta + 1)\ /2\sqrt{\mathrm{Y}_L^D}$) vs ($\sqrt{\mathrm{Y}_L^P}$ / $\sqrt{\mathrm{Y}_L^D}$) to obtain the two components of SFE ($\mathrm{Y}_S^D$) and polar ($\mathrm{Y}_S^P$) for the solid surface.

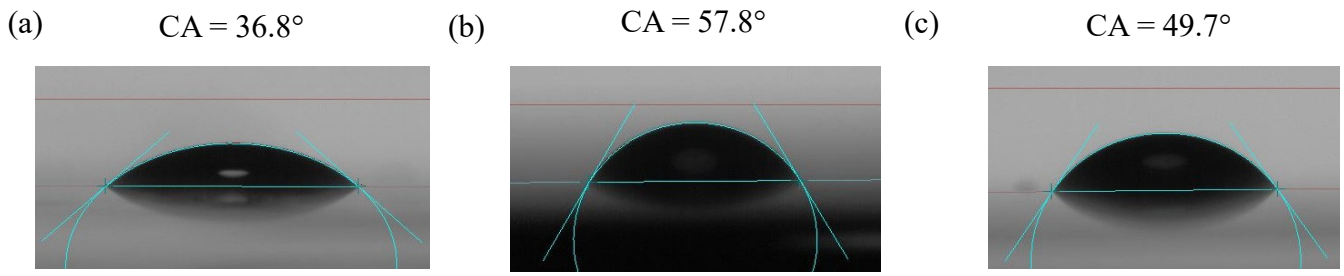


**Figure S6.** Contact angles of (a) Diiodomethane (b) Ethylene glycol & (c) Formamide on the PET substrate.

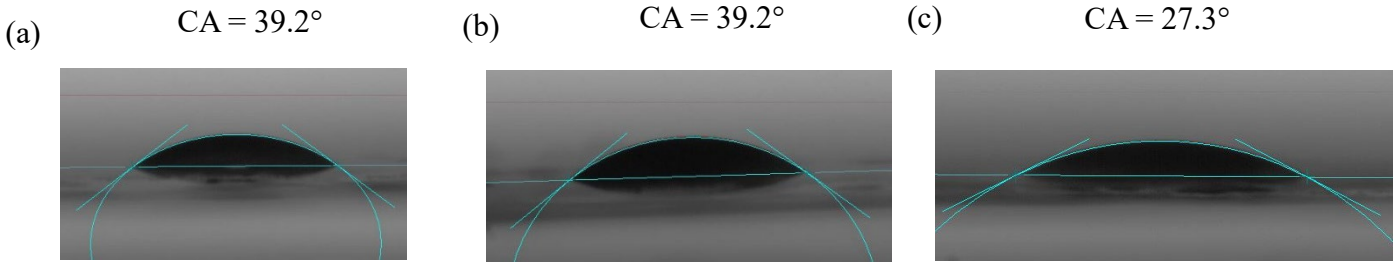


**Figure S7.** Contact angles of (a) Diiodomethane (b) Ethylene glycol & (c) Formamide on PVA coated PET substrate.

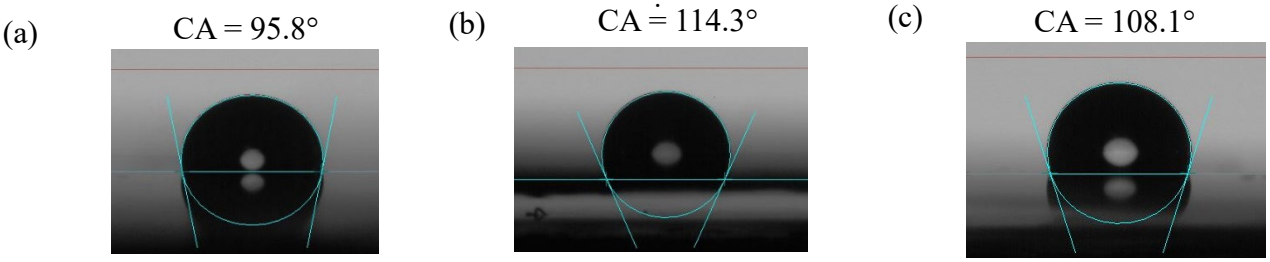


**Figure S8.** Contact angles of (a) Diiodomethane (b) Ethylene glycol & (c) Formamide on NeverWet coated PET substrate.

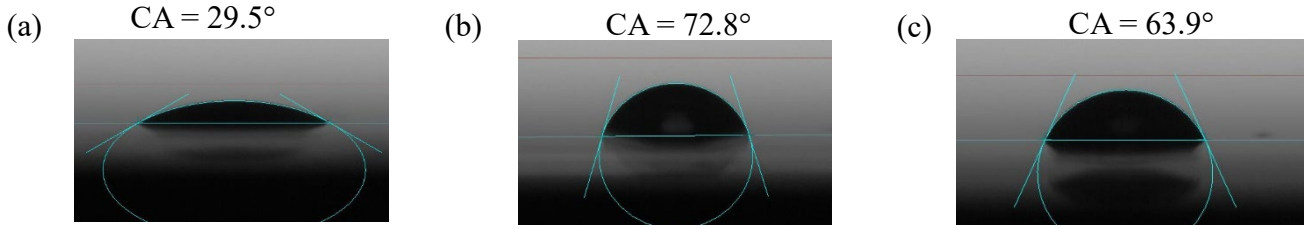


**Figure S9.** Contact angles of (a) Diiodomethane (b) Ethylene glycol and (c) Formamide on the CLC film.

**Analysis of the CLC alignment structure during the DIW process**

The Weissenberg number is defined as: $Wi = \lambda\dot{\gamma}$,[S6] where $\lambda$ is the material relaxation time constant for the ink, and $\dot{\gamma}$ is the shear rate. Based on the Carreau fluid model,[S7] the local ink viscosity can be described as:

$$\eta = \eta_0[1 + (\lambda\dot{\gamma})^2]^{\frac{n-1}{2}} \quad (4)$$

Where, $\eta_0$ is the zero-shear viscosity, $n$ is the flow behavior index. The CLC viscosity at 70 °C (Figure 2a) is fitted using the Carreau model to obtain the three parameters of $\eta_0$, $\lambda$, and $n$ to be 5.944 Pa·s, 8.467 s, and 0.287, respectively. **Figure S10** shows the CLC viscosity at 70 °C and the fitted function.

During printing, the maximum shear rate at the nozzle walls is calculated by:[S6]

$$\dot{\gamma}_{max} \approx \frac{3n+1}{4n} \cdot \frac{32\dot{Q}}{\pi d_N^3} \quad (5)$$

Where, $\dot{Q} = v\pi d_N^2/4$; $v$ is the ink extrusion velocity; and $d_N$ is the nozzle inner diameter. For the CLC printing condition used in this study, i.e., printing velocity of 1 mm/s and nozzle inner diameter of 200 μm, $Wi_{max} = 549.3$, which is much larger than 1, indicating the structure of dominant monodomain.[S6]

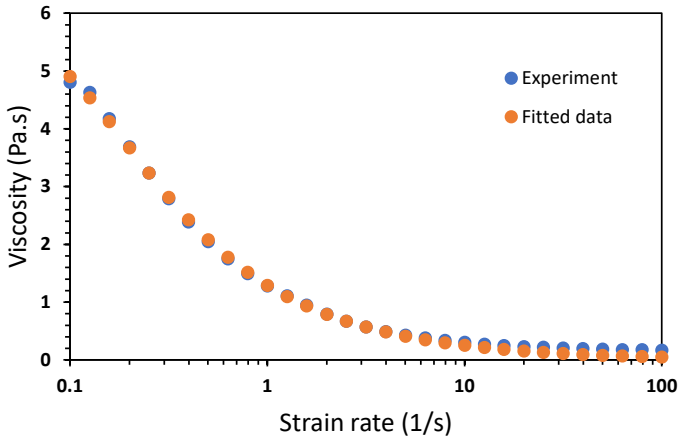


**Figure S10.** Fitted viscosity using the Carreau model.

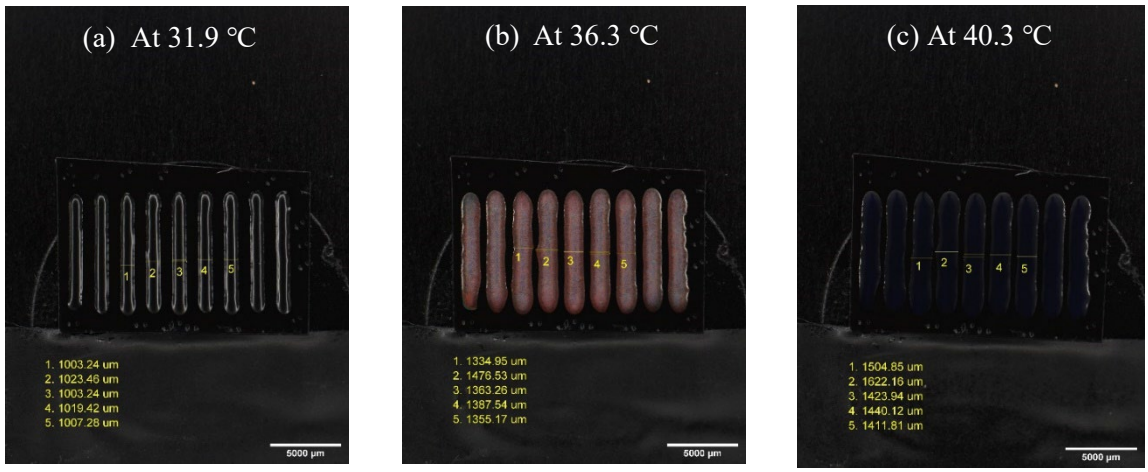


**Figure S11.** Spreading of CLC lines on the PET substrate during the first cycle of heating.

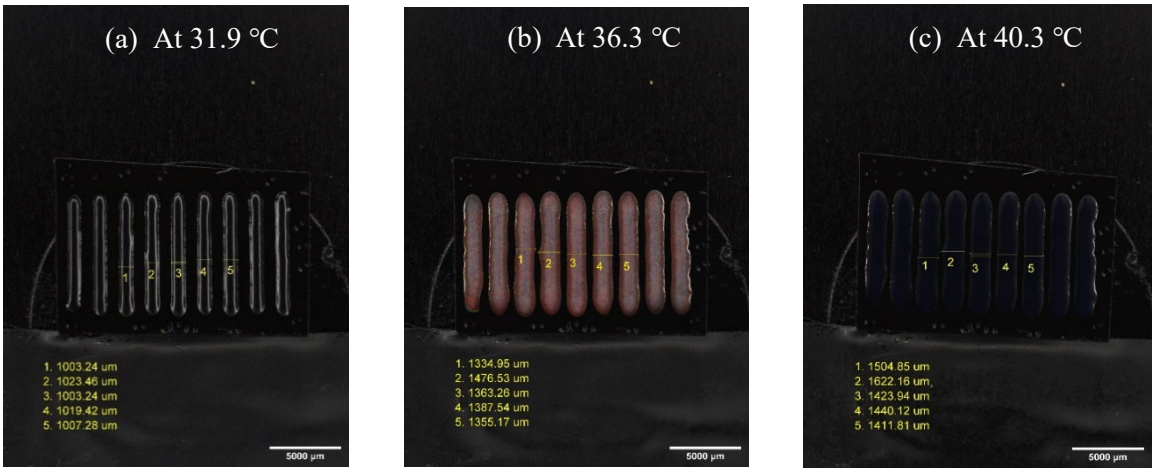


**Figure S12.** Spreading of CLC lines on the PVA coated-PET substrate during the first cycle of heating.

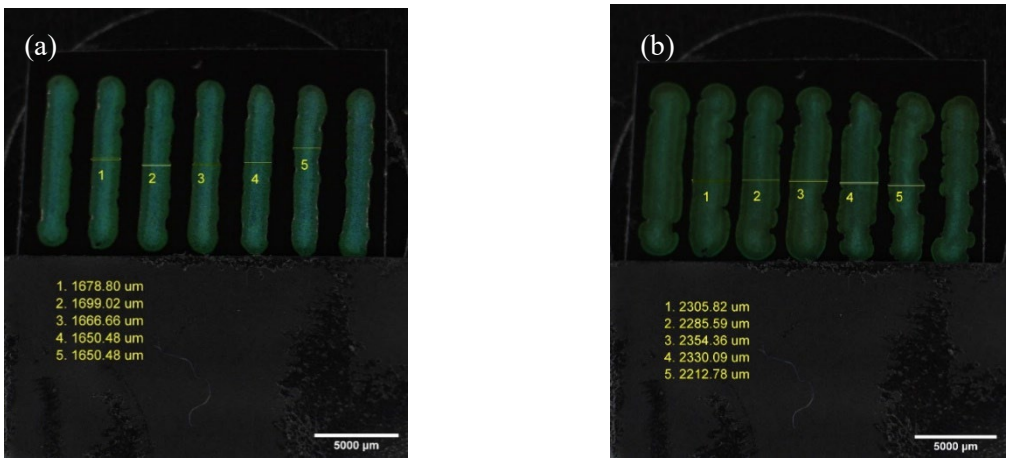


**Figure S13.** Spreading of CLC lines on the PVA coated-PET substrate after (a) the first; and (b) the tenth heating cycles, with line width measured at 37.3 ℃.

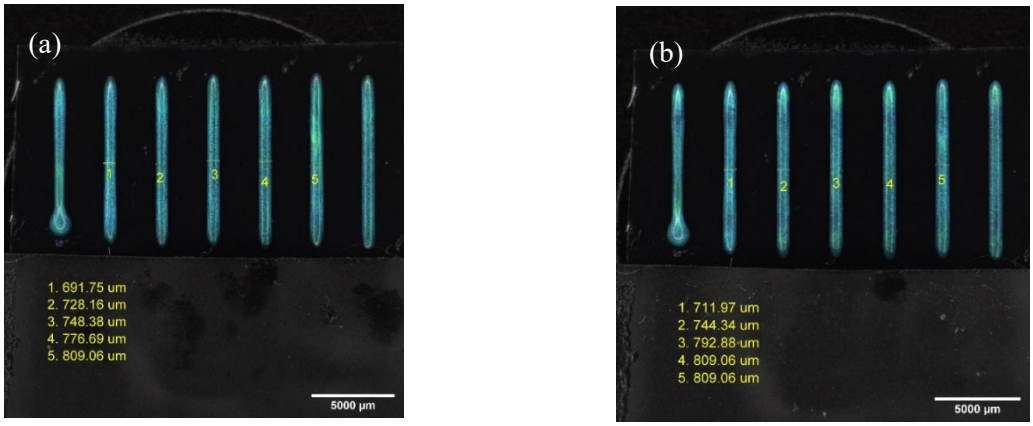


**Figure S14.** Spreading of CLC lines on the NeverWet coated-PET substrate after (a) the first; and (b) the tenth heating cycles, with line width measured at 37.3 ℃.

**References:**

S1 N. M. Sadiq, S. B. Aziz and M. F. Z. Kadir, *Gels*, 2022, **8**, 1–23.

S2 E. Olewnik-Kruszkowska, M. Gierszewska, E. Jakubowska, I. Tarach, V. Sedlarik and M. Pummerova, *Polymers (Basel).*, 2019, **11**, 2093.

S3 Y. Yang, H. Zhang, L. Cao, W. Meng, X. Ma, X. Li, J. Zheng and X. Liu, *J. Appl. Polym. Sci.*, 2024, **141**, 1–12.

S4 J. D. Brassard, D. K. Sarkar and J. Perron, *Appl. Sci.*, 2012, **2**, 453–464.

S5 H. Zhao, K.Y. Law, *Surface Wetting: Characterization, Contact angle, and Fundamentals*, Springer, 2016, **41**.

S6 R. Telles, A. Kotikian, G. Freychet, M. Zhernenkov, P. Wąsik, B.M. Yavitt, J.L. Barrera, C.C. Cook,

R. Pindak, E.C. Davidson and J.A. Lewis, *Proc. Natl. Acad. Sci,* 2025, **122,** 3.

S7 S. Bhatti, M. Zahid, R. Ali, A. Sarwar and H. A. Wahab, *Math. Comput. Simul.*, 2021, **190**, 659–677.